Lighting Res. Technol. 2021; **53**: 171–184

The Society of Light and Lighting

Light reflection spectra as a tool for direct and real-time determination of biomass and pigments in the microalgae *Microchloropsis salina*

Trinh Quang Vinh PhD[a], **Tran Nam Trung** PhD[b], **Jens Balasus** MSc[a], **Sulabha Sharma** PhD[b], **Tim Hegemann** MSc[a], **Simon Greulich** BSc[b], **Tran Quoc Khanh** PhD[a] and **Ralf Kaldenhoff** PhD[b]
[a]Laboratory of Lighting Technology, Technical University Darmstadt, Darmstadt, Germany
[b]Department of Biology Applied Plant Sciences, Technical University Darmstadt, Darmstadt, Germany

Received 22 April 2020; Revised 13 August 2020; Accepted 18 August 2020

To meet the increasing demand for mass-produced microalgae, production processes must be optimised and monitored. The herein described optical sensors provide an instantaneous and direct opportunity to monitor biological and biochemical information for microalgae cultivation. Combination of expertise in natural science and engineering, as well as the application of novel data acquisition and analysis methods, are required to develop an appropriate system for industrial purpose. Prior to this, the correlation between biological and physical parameters must be determined. In this work, we combined colour science with the experimentally determined dataset from the cultivation of *Microchloropsis salina*. Our results indicate a resilient correlation between algal biomass and its specific pigment concentration with the determined reflection spectrum. Data evaluation allowed us to establish identification models for contactless quantification of the respective biological parameter in large-scale automated bioreactors.

1. Introduction

Derived from the Latin word '*alga*' (seaweed), algae is the common name for an extremely diverse group of aquatic photosynthetic organisms. Many algae show a large economic potential. Rich in both nutrients and vitamins, algae have long been recognised as a promising alternative food source that could help mankind to overcome the challenges of food shortage and overpopulation.[1] Several algal species have been established as highly demanded dietary and nutraceutical products, with annual production rates in the range of thousands of metric tons.[2] Algae are also capable of biosynthesising various high-value bioproducts such as carotenoids,[3–5] polyunsaturated fatty acids,[6] polysaccharides[7] and bioactive compounds.[8] The oil industry is equally interested in algae due to their ability to accumulate large amounts of lipids, which could be turned into biofuel and biodiesel.[9]

Effective cultivation of algae requires easily accessible data of biomass, cell size, cell number, cell morphology and concentration of biochemical ingredients. Measurements of

Address for correspondence: Trinh Quang Vinh, Laboratory of Lighting Technology, Technical University Darmstadt, Darmstadt 64289, Germany.
E-mail: vinh@lichttechnik.tu-darmstadt.de

10.1177/1477153520958455

optical density (*OD*) and automated cell counting have been established as reliable methods to quantify biomass or cell number.[10,11] Characterisation and quantification of bioproducts, on the other hand, still rely on laborious, expensive, time-consuming, destructive analytical methods such as high-performance liquid chromatography (HPLC), which exclude the possibility of real-time monitoring. In this context, optical contactless measurement (OCM) appears as an attractive alternative to the conventional methods as it allows rapid, non-destructive measurements at only a fraction of the cost. In agriculture, OCM has been applied in the measurement of chlorophyll or nitrogen status,[12] fruit maturity identification,[13] detection of diseases[14] or diverse stresses.[15]

Also, some OCM techniques are successfully used for algae, including confocal Raman microscopy,[16,17] Fourier-transform infrared spectroscopy,[17] as well as measurements of fluorescence[18] or absorption.[19] Measurement of reflectance spectra is another popular OCM technique that has key advantages. One of the first applications of reflectance analysis for algae was the monitoring and control of toxic oceanic algal blooms.[20] Another application is taxonomic characterisation: key differences in reflectance spectra allowed Gitelson *et al.*[21] to distinguish between species of four important microalgal phyla (Chlorophyta, Cyanophyta, Bacillariophyta and Pyrrophyta). Reflectance measurements could also be used for algal growth monitoring in bioreactors.[22]

Algae are highly suitable for reflectance measurements because they produce large quantities of pigments. Furthermore, many algal pigments are valuable and highly sought pharmaceutical/nutraceutical products. The colour nature of an algae sample contains information of not only its biomass but also its pigment contents – parameters that are of great economic interest. The application of reflectance measurement in large-scaled cultivation also renders obsolete the employment of conventional chemical analysis procedures on small, precious biological samples, which are laborious to obtain with destructive extraction methods and reliant on expensive and bulky equipment. In contrast, the spectral reflectance measurement can be implemented online, direct and immediate, thus opening the opportunity of real-time monitoring, controlling and optimisation. Accurate and reliable spectral data for each spectral band of the complete spectral power distribution can be obtained with high-cost spectrometers. In case of the establishment of accurate identification models, the spectrometer can be replaced by a more affordable sensor chip. By this, economic device design can meet technical benefit. With the approach described herein for the establishment and application of an identification model, cultivation optimisation combined with specific ingredient optimisation can be feasible in modern massive industrial applications.

Despite these advancements and considerations, the usage of OCM in the production of industrially relevant algae remains, in parts, a *terra incognita*. By this pre-feasibility study, we aim to establish the basis for a new identification model that could be applied to large-scale automatic algal farms by combining biological parameters regarding the microalga *Microchloropsis salina* with its colour science properties to reveal possible correlations between these two datasets. Instead of expensive and time-consuming chromatography techniques, this new method will rely solely on colour analysis for biological predictions and quantifications, thus enabling the real-time simultaneous monitoring of diverse biological and biochemical parameters at very low cost.

2. Algae cultivation and measurements of biological parameters: Experiments and results

We used the *Microchloropsis salina* strain *SAG 40.85*[23] for experiments. Algal cells were

maintained on agar solidified SWES medium.[24] Unless stated otherwise, cells were cultivated in liquid SWES medium without soil extract. Prior to the main experiment, 25 mL of pre-culture were inoculated with cells from agar plates and cultivated for seven days on a horizontal shaker at 90 r/min at room temperature and under constant top illumination of 80 µmol/m^{2}s white light. Subsequently, the algal culture was transferred to a bubble column bioreactor with a volume of 500 mL and cultivated for another seven days under continuous lateral illumination of 80 µmol/m^{2}s white light. Agitation was provided by a constant stream of pressurised air enriched with 2% of CO_2. At the end of the two-week period, the optical density at 680 nm (*OD680*) of the pre-culture reached 13.

Algal cultivation was carried out in four independent bubble column bioreactors with a volume of 500 mL each (Figure 1). Agitation was provided by a constant stream of pressurised air enriched with 2% of CO_2. Illumination was provided by a mixture of light-emitting diodes (LED) of different colours – white (3200 K), violet (405 nm), blue (465 nm), green (515 nm), yellow (593 nm) and red (630 nm) (Figure 1), whereby two cultures (M_1 and M_2) were illuminated with low light intensity of 50 µmol/m^{2}s and the other two (M_3 and M_4) with high light intensity of 150 µmol/m^{2}s. Ambient temperature was maintained at 25°C. The pre-culture was used to inoculate the new bioreactors; the starting *OD680* of all four bioreactors was 0.646. We defined the start of the cultivation as Day 1 (D_1); 10 mL of samples were taken at

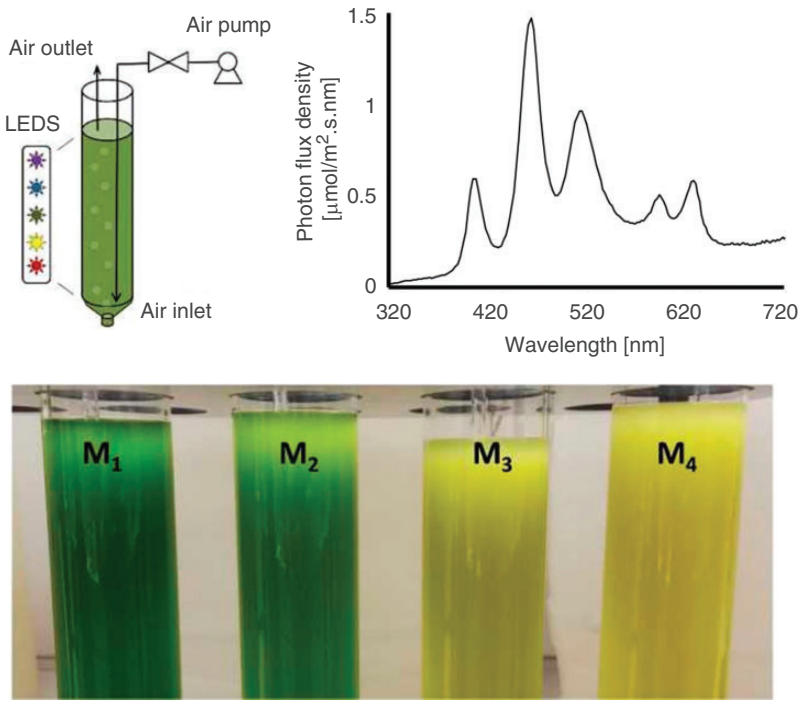

Figure 1 (Upper left) Schematic diagram of a bubble column used for algal cultivation. (Upper right) Spectrum of illuminating LEDs. (Lower) Algal cultures at Day 9. From left to right: M_1, M_2, M_3, M_4

Day 1 (D_1), Day 4 (D_4), Day 5 (D_5), Day 8 (D_8) and Day 9 (D_9) for determination of *OD680* and pigment concentration.

The *OD680* values were measured by measuring the absorbance of the algal suspensions at 680 nm with a spectrophotometer. Quantification of two main pigments of *Microchloropsis salina* – chlorophyll A (green) and carotenoids (orange) – was carried out as follows: 1 mL of sample was transferred to a 1.5 mL screw-cap Eppendorf tube and centrifuged for 5 minutes at 10 000 r/min. The supernatant was removed, and 1 mL methanol and 0.1 g glass beads (0.5 mm in diameter) were added. The cells were subsequently mechanically disrupted in a Benchmark Bead Blaster 24 homogeniser (four 10-s cycles at 7 m/s^2 with 10-s pause in between), and the pigments were extracted into methanol. The pigment-containing methanol phase was separated from cell debris by centrifugation at 10 000 r/min for 10 minutes and then transferred to a fresh Eppendorf tube. Pigment extraction was repeated until the pellet was white. In the next step, we determined the absorbance (A) at 665 nm, 652 nm and 480 nm of the methanol extract, using a spectrophotometer. Concentrations of chlorophyll A and carotenoids can be calculated as follows[25]

$$Chlorophyll\ A\left[\mu\frac{g}{mL}\right] = 16.5169 \times A665\,nm - 8.0962 \times A652\,nm \quad (1)$$

$$Total\ carotenoids\left[\mu\frac{g}{mL}\right] = 4 \times A480\,nm \quad (2)$$

The development of OD680, chlorophyll A concentration and total carotenoid concentration throughout the cultivation period are presented in Figure 2. While the curves of batches which were cultivated under the same conditions – M_1 compared to M_2 and M_3 compared to M_4 – were relatively similar, there were remarkable differences between M_1, M_2 (low-light group) and M_3, M_4 (high-light group) in all three parameters. Under low-light conditions, the rates of biomass production (represented by the slope of *OD680* curves) were higher than under high-light conditions. On the other hand, more pigments were produced under high light than in low light. These differences led to easily recognisable differences in colours. At the end of the cultivation (Day 9), M_1 and M_2 appeared bright green, while M_3 and M_4 were yellow (Figure 1).

3. Description of the optical measurement system and results

3.1 Optical measurement system

The measurement system included (1) a spectrometer camera CS2000 of Konica Minolta – *CS*,[26] (2) a white standard of SphereOptics – WST[27] and (3) a stable

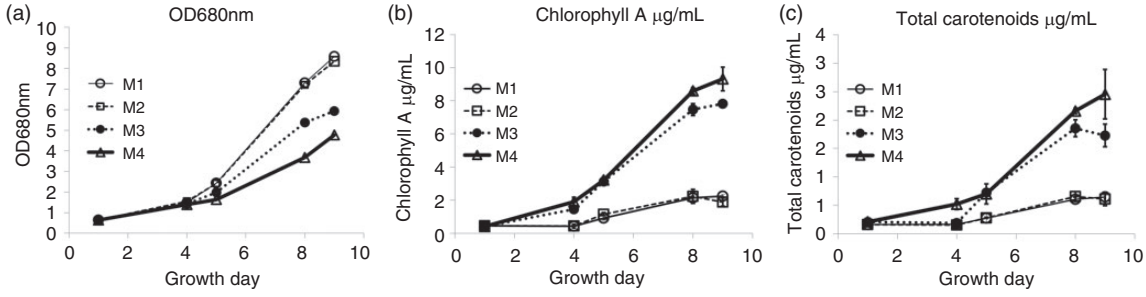

Figure 2 Developments of OD680, green pigment chlorophyll A and orange pigment carotenoids of M_1 – M_4 throughout the cultivation period

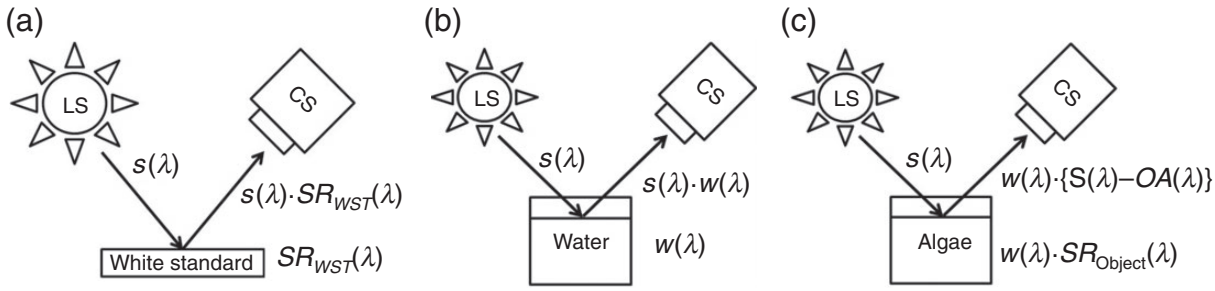

Figure 3 Measurement procedure and system for the spectral reflectance of microalgae

tungsten halogen lamp – *LS*. The task of the CS2000 was to measure the absolute spectral radiance distributions so that the colour properties described completely by spectral reflectance of measurement objects could be determined. The white standard provided excellent spectral reflectance ($SR_{\mathrm{WST}}(\lambda)$ with wavelength λ in nm). This spectral reflectance is nearly 100% in the complete visible wavelength from 380 to 780 nm; it was previously provided by SphereOptics. The task of this white standard was to support data for the comparison between its spectral reflectance and the one of the measured objects. The stable tungsten halogen lamp (*LS*) played an important role at it provided a stable absolute spectral power distribution ($S(\lambda)$). Its spectrum must be constant during measurement and is not dependent on temperature, time and other factors; therefore, spectral changes achieved from the measurements resulted from the measured objects and their biological/optical properties only.

Another aspect of the measurement procedure, the optical determination, can be classified into the three elements (1) measurement with white standard, (2) measurement with water and (3) measurement with microalgae culture. In detail, the product of the tungsten halogen lamp spectrum ($S(\lambda)$) and spectral reflectance ($SR_{\mathrm{WST}}(\lambda)$) was measured by CS2000; $SR_{\mathrm{WST}}(\lambda)$ has been provided by the supplier. Therefore, the spectral power distribution can be determined by equation (3)

$$S(\lambda) = \frac{S(\lambda) \cdot SR_{\mathrm{WST}}(\lambda)}{SR_{\mathrm{WST}}(\lambda)} \tag{3}$$

Similarly, the optical properties of the water ($W(\lambda)$) can be computed by the division between the measured product $S(\lambda)$ and $W(\lambda)$ by CS2000 and the determined spectral power distribution $S(\lambda)$, following equation (4)

$$W(\lambda) = \frac{S(\lambda) \cdot W(\lambda)}{S(\lambda)} \tag{4}$$

The product of the water's optical property $W(\lambda)$ and the subtraction between spectral power distribution $S(\lambda)$ and the spectral absorption of the measurement objects ($OA(\lambda)$) can be measured by CS2000, while $W(\lambda)$ is known. The spectral reflectance of the measurement objects ($SR_{\mathrm{Object}}(\lambda)$) is the product divided by $W(\lambda)$, as in equation (5)

$$SR_{\mathrm{Object}}(\lambda) = \frac{W(\lambda) \cdot \{S(\lambda) - OA(\lambda)\}}{W(\lambda)} \tag{5}$$

The spectral reflectance determined in equation (2) is the function of growth and biological ingredients of the measurement objects. In the case of this study, they are the microalgae samples. Consequently, the

spectral absorption of the measurement objects can also be determined by subtraction of the spectral power distribution $S(\lambda)$ and spectral reflectance $SR_{\text{Object}}(\lambda)$, following equation (6)

$$OA(\lambda) = S(\lambda) - SR_{\text{Object}}(\lambda) \tag{6}$$

Spectral absorption comprises many components such as the absorption of pigments and other components. The absolute exact determination of all components is quite complex. However, within the limits of our identification models, we considered only the approximately spectral absorption of the specific pigments for further calculations.

3.2 Raw optical measurement results and discussion

The basis of the measurement system and principle is given in detail in section 3.1. The microalgae samples under two different cultivation conditions, as depicted in section 2, were measured. Herewith, the spectral reflectance values in Figure 4 are those of the same microalgae samples under different growth days. The standard daylight spectrum 6500 K under the view angle 2° was selected to create the appropriate colour appearances corresponding with the true colours of the microalgae samples with different growth days and cultivation conditions in the experiments.

Based on Figure 4, the microalgae samples showed similar growth tendencies. On the first day, the colours of the different samples were nearly similar, i.e. dark grey, reflecting the colour of the culture medium. Subsequently, over the following days, the samples strongly absorbed blue short wavelengths (from about 400 to 480 nm; peak at approximately 80–99%) and red long wavelengths (from about 650 to 700 nm; maximum at 60–99%). However, the different spectral changes of two microalgae groups conditioned under two brightness levels ($M_1 - M_2$ as low photosynthetic photon flux in 50 µmol/m^{2}s and $M_3 - M_4$ as high photosynthetic photon flux in 150 µmol/m^{2}s) could be reliably identified. Under low photosynthetic photon flux, the spectral absorption of M_1 and M_2 in both the blue and the red range was weaker (maxima of approximately 99% for

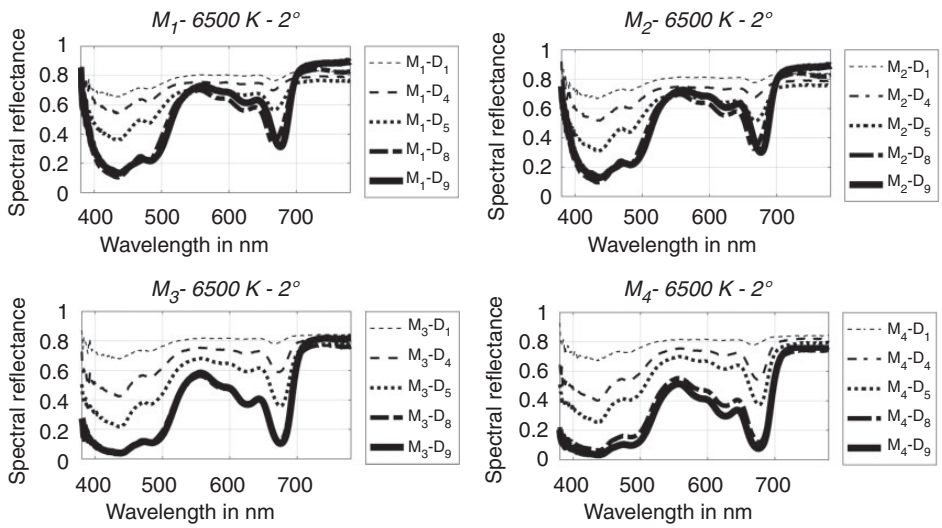

Figure 4 Spectral reflectance in the case of similar microalgae and different growth days
CCT: colour correlated temperature

blue and 70% for red). In addition, the spectral reflectance values of the green–yellow–orange middle wavelength were also quite flat, with small spectral fluctuations. These findings are consistent with the lower contents of chlorophyll A and carotenoids in M_1 and M_2.

4. Fine colour processing and identification models based on colour science

4.1 The growth identification model based on colour shift Δxy

In Figure 2, the relationships between growth and *OD680*, chlorophyll A and carotenoids in the growth process of microalgae samples are depicted. Based on the spectral measurement in section 2, spectral changes of microalgae reflectance were identified and are displayed in Figure 4 regarding the lighting technique. The main question was how to combine these so that only basic parameters of simple measurable colour indices, which can be provided by an inexpensive colour sensor, could aid to quantify the growth index *OD680*.

When the microalgae samples (characterised by spectral reflectance $SR_{\text{Microalgae}}(\lambda)$) were illuminated by a daylight source ($DL_{6500}(\lambda)$ with wavelength λ in nm) with the correlated colour temperature (*CCT* in K) of 6500 K and a view angle of 2° (denoted by the colour matching function x_2, y_2 and z_2), their natural colours could be observed visually, as shown in Figure 4. Based on colour science, they can be converted into chromaticity (x, y) in the colour diagram xy in Figure 5. Herewith, the chromaticity x and y can be calculated as follows[28–31]

$$X = \int_{380}^{780} DL_{6500}(\lambda) \cdot SR_{\text{Microalgae}}(\lambda) \cdot x_2(\lambda) \cdot \mathrm{d}\lambda \tag{7}$$

$$Y = \int_{380}^{780} DL_{6500}(\lambda) \cdot SR_{\text{Microalgae}}(\lambda) \cdot y_2 \cdot (\lambda) \cdot \mathrm{d}\lambda \tag{8}$$

$$Z = \int_{380}^{780} DL_{6500}(\lambda) \cdot SR_{\text{Microalgae}}(\lambda) \cdot z_2(\lambda) \cdot \mathrm{d}\lambda \tag{9}$$

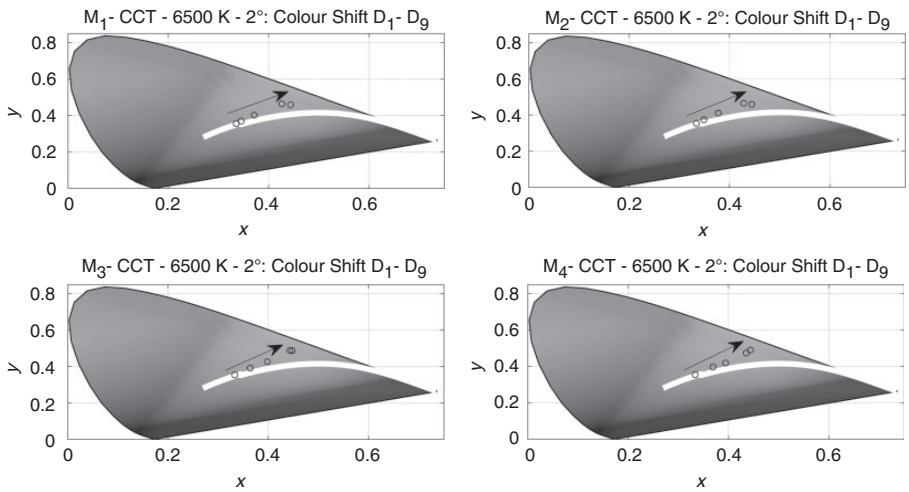

Figure 5 Colour shifts of microalgae sample under different growth days
CCT: correlated colour temperature.

$$x = \frac{X}{X+Y+Z} \quad (10)$$

$$y = \frac{Y}{X+Y+Z} \quad (11)$$

As a result, from the first to the final growth day, the natural colours of the microalgae samples changed from the centre of the colour diagram xy to its boundary in the direction of colour saturation. These colour shifts are quite similar qualitatively and nonlinear, but saturated at a point. Both the speed of the change and saturation point were different according to growth days and microalgae samples.

Quantitatively, the output of colour sensors automatically supplies the chromaticity in time. Therefore, the colour difference in time can be determined as follows

$$\Delta xy(t) = \sqrt{(x_t - x_0)^2 + (y - y_0)^2} \quad (12)$$

where (x_0, y_0) and (x_t, y_t) are chromaticity at time t_0 and t, respectively. Δxy(t) is the colour difference in time compared with the start time. These colour difference functions are described in Figure 6 with the quadratic polynomial functions. The coefficient of determination (R^2) values of 0.988 or 0.99 prove that the quality of the correlations is significant and that the model can be applied as the expected identification model of the growth index *OD680* using colour shift in time.

4.2 Ingredient identification models using theoretical quantities of ChA and CaT

Equally important to the growth index *OD680* is the green pigment chlorophyll A. This index has commonly been determined with offline, time-consuming and destructive methods and devices in biology laboratories, as mentioned in the Results chapter and in Figure 2.

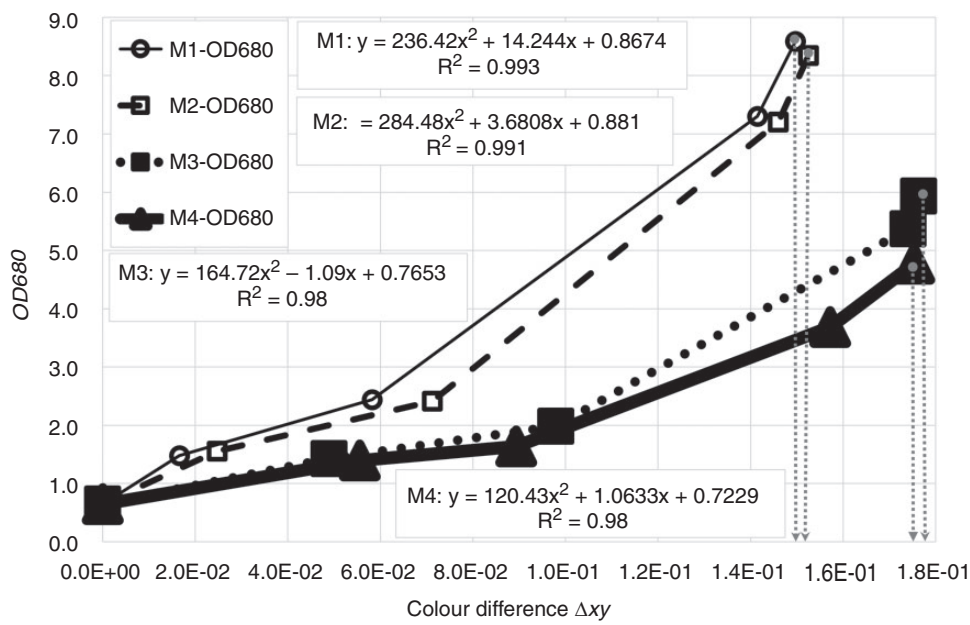

Figure 6 Identification models of the growth index OD680 using colour shift

With regard to lighting technique, if the luminaire of the microalgae lighting system is fixed with its absolute spectral power distribution ($SPD(\lambda)$), the effective absorption curve of chlorophyll A ($Chlorophyll\_A(\lambda)$) has previously defined as that in Figure 7 and the spectral reflectance values ($SR_{\text{Microalgae}}(\lambda)$) are shown in Figure 4, the integrated amount for a theoretical quantity of the green pigment chlorophyll A (ChA) can be determined as follows

$$ChA = \int_{380}^{780} SPD(\lambda) \cdot \{1 - SR_{\text{Microalgae}}(\lambda)\} \cdot \text{Chlorophyll\_A}(\lambda) \cdot d\lambda \tag{13}$$

To quantify the theoretical quantity of ChA in a real application and to keep the technical update with the newest innovation of horticulture lighting, we studied the optimal LEDs for horticulture lighting and spectral effect grade of valuable (beta carotene, chlorophyll A and chlorophyll B) ingredients based on the technical publication of the company LUMILEDS (lumileds.pnwsoft.com ©LUMILEDS[32,33]). The absolute spectral power distributions of the LEDs with a photon flux density higher than 53 μmol/s and a spectral effect grade are shown in Figure 7. The major peak wavelengths were in the blue short wavelength range (380–490 nm) and in the red long wavelength range (600–760 nm). Some LEDs were also supplemented with green–yellow–orange wavelengths (500–600 nm) and far red wavelengths.

The technical specifications of the common LEDs used in horticulture are listed in Table 1. They are the best up-to-date LED spectra that are necessary for Parameter $SPD(\lambda)$, used in equations (13) and (14). The results show that three LEDs (Deep Red, Pink and 25% Blue) are the best candidates depending on the evaluation parameters (photon flux density PPF in μmol/s and/or biological efficacy in μmol/J). In this

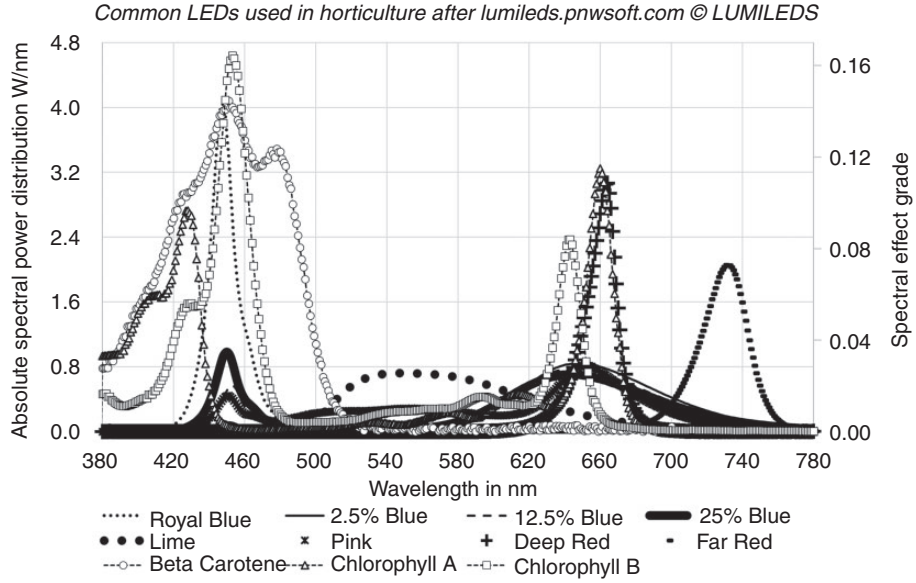

Figure 7 Optimal LEDs for horticulture lighting and spectral effect grade of valuable (beta carotene, chlorophyll A and chlorophyll B) ingredients after lumileds.pnwsoft.com ©LUMILEDS[32,33]

work, LED Pink was selected because it has the highest photosynthetic photon flux in the wavelength range 400–700 nm ($PPF_{PAR,400–700} = 87.36\,\mu mol/s$), while other parameters are not low compared to the other two LEDs.

In Figure 8 (left), the longer the growth day, the higher the chlorophyll A amount (μg/mL) and the higher the theoretical quantity (*ChA*). Based on the clear tendency, the identification models of the green pigment chlorophyll A, using Quantity *ChA*, are constructed like the curves and the quadratic polynomial functions in Figure 8 (right). The coefficient of determination (R^2) values of 0.90 to 0.99 confirm that the quality of the correlations is very good and that the models can be applied as the expected identification models of the green pigment chlorophyll A using Quantity *ChA*.

Similarly, the integrated amount for a theoretical quantity of the yellow pigments carotenoids (*CaT*) can be determined as follows

$$CaT = \int_{380}^{780} SPD(\lambda) \cdot \{1 - SR_{Microalgae}(\lambda)\} \cdot \text{Carotenoids}(\lambda) \cdot d\lambda \tag{14}$$

Table 1 Technical specification of the common LEDs used in horticulture after lumileds.pnwsoft.com ©LUMILEDS[32,33]

Part number	P_{el} (W)	$PPF_{Total,380–850}$ (μmol/s)	$PPF_{PAR,400–700}$ (μmol/s)	Efficacy $\eta_{PAR,400–700}$ (μmol/J)	Efficacy $\eta_{Total,380–850}$ (μmol/J)
Deep Red	**28.896**	**67.8**	**67.2**	**2.33**	**2.35**
Far Red	28.896	**71.85**	**4.17**	**0.14**	**2.49**
Lime	40.32	**92.1**	**89.6**	**2.22**	**2.28**
Pink	**38.304**	**93.83**	**87.36**	**2.28**	**2.45**
2.5% Blue	38.304	**86.54**	**70.56**	**1.84**	**2.26**
12.5% Blue	38.304	**91.94**	**78.4**	**2.05**	**2.40**
25% Blue	**38.304**	**95.78**	**82.88**	**2.16**	**2.50**
Royal Blue	40.32	**83.39**	**82.88**	**2.06**	**2.07**

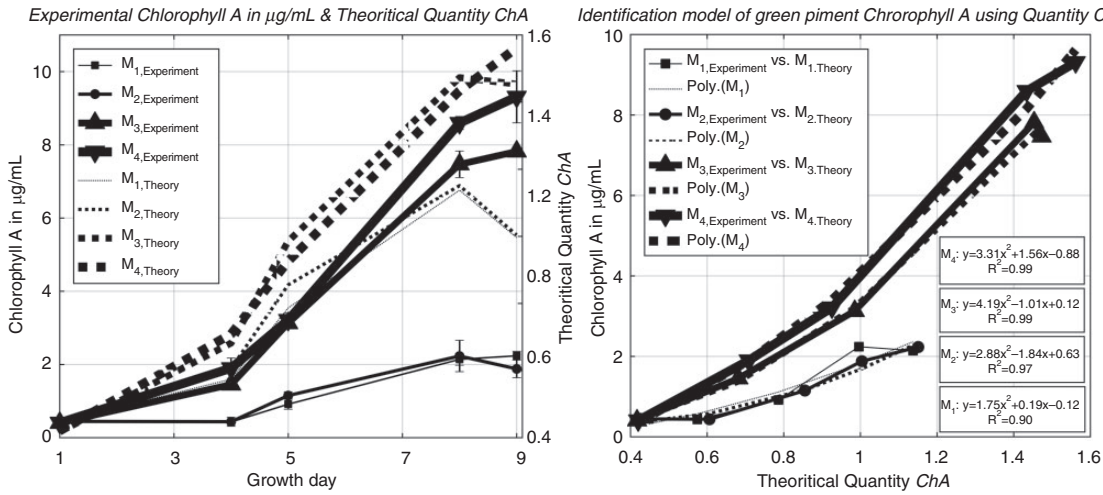

Figure 8 Identification model of the green pigment chlorophyll A using Quantity ChA

where carotenoids(λ) is the effective absorption curve of carotenoids, as defined.

The tendencies of experimental and theoretical values in Figure 9 (left) were relatively similar compared to those shown in Figure 8 (left), although their magnitude was lower and the standard deviation was higher. Consequently, the identification models of the yellow carotenoids using Quantity *CaT* can be built as in Figure 9 (right).

5. Conclusions and future works

In this work, the expertise of two groups working in natural science and in engineering science was combined to develop the basis for a new measurement system capable of monitoring growth and pigment production in green algae. Over nine days, *Microchloropsis salina* samples were cultivated under two different lighting conditions (M_3 and M_4 under 150 µmol/m^{2}s and M_1 and M_2 under 50 µmol/m^{2}s). The higher photosynthetic photon flux resulted in lower biomass but better pigment production. These findings confirm the well-known fact that light is an important regulatory factor in algae biology and metabolism.[34] Via comparison of reflectance spectra, we were able to clearly distinguish the high light group (M_3 and M_4) from the low light group (M_1 and M_2), thus demonstrating the potential applications of reflectance analysis both in algae-light-interaction research as well as in lighting optimisation for algal production.

The nature of the colour properties by spectral reflectance can be measured precisely by a modern spectrometer. The results helped to determine the colour shift of microalgae samples over time. Consequently, growth identification models using colour shift Δxy were developed, with a good correlation to algae growth rates. Once the models are developed in more detail, low-cost colour sensors[35,36] can replace the spectrometer to design inexpensive devices. More sophisticated ingredient identification models using theoretical quantities *ChA* and *CaT* are also proposed. We observed good correlations of *ChA* and *CaT* to the practically determined contents of

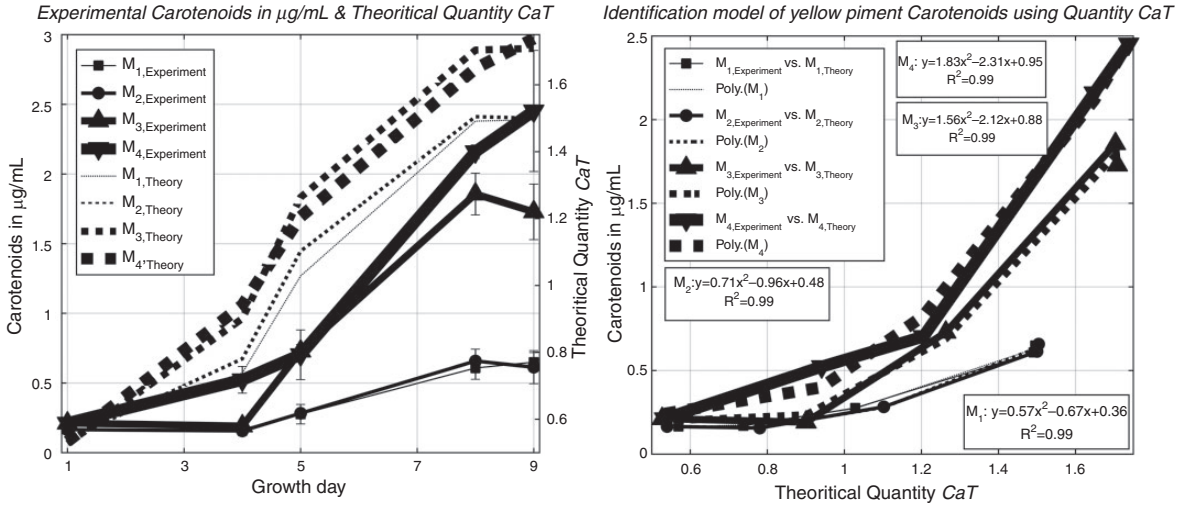

Figure 9 Identification model of the yellow pigment carotenoids using Quantity CaT

corresponding green and yellow pigments (chlorophyll A and carotenoids). Our results indicate that it is possible to calculate biomass and the specific pigment concentration of an algal culture based solely on its colour properties. Such correlations form the important starting point for the establishment of models applicable for microalgae cultivation.

As a pre-feasibility study, this work revealed the large potential of the cooperation between biological and colour research. The obtained identification models are of real interest for the monitoring and optimisation of large-scaled automated microalgae cultivations. Nevertheless, the robustness and accurateness of our models still needs to be verified in extensive testing with larger amounts of samples and greater variations of biological conditions. The usefulness of our models for the prediction of other biological and biochemical parameters also requires further studies. These points will be addressed in our future works.

Declaration of conflicting interests

The authors declared no potential conflicts of interest with respect to the research, authorship, and/or publication of this article.

Funding

The authors received no financial support for the research, authorship, and/or publication of this article.

ORCID iD

Trinh Quang Vinh https://orcid.org/0000-0002-1390-5322

References

1 Belasco W. Algae burgers for a hungry world? The rise and fall of *Chlorella* cuisine. *Technology and Culture* 1997; 38: 608–634.
2 Guccione A. *Chlorella* for protein and biofuels: from strain selection to outdoor cultivation in a Green Wall Panel photobioreactor. *Biotechnology for Biofuels* 2014; 7: 84.
3 Borowitzka MA. Dunaliella: biology, production, and markets. In *Handbook of Microalgal Culture Applied Phycology and Biotechnology*, 2nd Edition. Wiley, 2013. DOI: 10.1002/9781118567166.ch18.
4 Olaizola M, Huntley ME. Recent advances in commercial production of astaxanthin from microalgae. In *Recent Advances in Marine Biotechnology*, Volume 9. New Hampshire: Biomaterials and Bioprocessing Science Publishers, 2003, pp. 143–164.
5 Mikami K, Hosokawa M. Biosynthetic pathway and health benefits of fucoxanthin, an algae-specific xanthophyll in brown seaweeds. *International Journal of Molecular Sciences* 2013; 14: 13763–13781.
6 Pereira H, Barreira L, Figueiredo F, Custódio L, Vizetto-Duarte C, Polo C, Rešek E, Engelen A, Varela J. Polyunsaturated fatty acids of marine macroalgae: potential for nutritional and pharmaceutical applications. *Marine Drugs* 2012; 10: 1920–1935.
7 Tannin-Spitz T, Bergman M, Van-Moppes D, Grossman S, Arad SM. Antioxidant activity of the polysaccharide of the red microalga *Porphyridium* sp. *Journal of Applied Phycology* 2005; 17: 215–222.
8 Li S, Ji L, Shi Q, Wu H, Fan J. Advances in the production of bioactive substances from marine unicellular microalgae *Porphyridium* spp. *Bioresource Technology* 2019; 292: 122048.
9 Borowitzka MA. Algae oils for biofuels: chemistry, physiology, and production. In *Single Cell Oils: Microbial and Algal Oils*, 2nd Edition. Elsevier, 2010, pp. 271–289.
10 Fei J, Murat K, Kimberly LO. Multi-wavelength based optical density sensor for autonomous monitoring of microalgae. *Sensors* 2015; 15: 22234–22248.

11 Toshiyuki T. Applicability of automated cell counter with a chlorophyll detector in routine management of microalgae. *Scientific Reports* 2018; 8: 4967.
12 Haboudane D, Miller JR, Tremblay N, Zarco-Tejada PJ, Dextraze L. Integrated narrow-band vegetation indices for prediction of crop chlorophyll content for application in precision agriculture. *Remote Sensing of Environment* 2002; 81: 416–426.
13 Rajkumar P, Wang N, EImasry G, Raghavan GSV, Gariepy Y. Studies on banana fruit quality and maturity stages using hyperspectral imaging. *Journal of Food Engineering* 2012; 108: 194–200.
14 Bauriegel E, Giebel A, Geyer M, Schmidt U, Herppich WB. Early detection of *Fusarium* infection in wheat using hyper-spectral imaging. *Computers and Electronics in Agriculture* 2011; 75: 304–312.
15 Sepulcre-Canto G, Zarco-Tejada PJ, Jiménez–Muñoz JC, Sobrino JA, de Miguel E, Villalobos FJ. Detection of water stress in an olive orchard with thermal remote sensing imagery. *Agricultural and Forest Meteorology* 2006; 136: 31–44.
16 Collins AM, Jones HD, Han D, Hu Q, Beechem TE, Timlin JA. Carotenoid distribution in living cells of *Haematococcuspluvialis* (Chlorophyceae). *PLoS One* 2011; 6: e24302.
17 Liu J, Huang Q. Screening of astaxanthin-hyperproducing *Haematococcuspluvialis* using fourier transform infrared (FT-IR) and Raman microspectroscopy. *Applied Spectroscopy* 2016; 70: 1639–1648.
18 Yentsch CS, Menzel DW. A method for the determination of phytoplankton chlorophyll and phaeophytin by fluorescence. *Deep Sea Research and Oceanographic* 1963; 10: 221–231.
19 Yacobi YZ, Köhler J, Leunert F, Gitelson A. Phycocyanin-specific absorption coefficient: eliminating the effect of chlorophylls absorption. *Limnology and Oceanography: Methods* 2015; 13: e10015.
20 Blondeau-Patissier D, Gower JFR, Dekker AG, Phinn SR, Brando VE. A review of ocean colour remote sensing methods and statistical techniques for the detection, mapping and analysis of phytoplankton blooms in coastal and open oceans. *Progress in Oceanography* 2014; 123: 123–144.
21 Gitelson AA, Schalles JF, Rundquist DC, Schiebe FR, Yacobi YZ. Comparative reflectance properties of algal cultures with manipulated densities. *Journal of Applied Phycology* 1999; 11: 345–354.
22 Thomas AR, Aaron MC, Omar FG, Anne MR, Howland DTJ, Jerilyn AT. Spectroradiometric monitoring of *Nannochloropsis salina* growth. *Algal Research* 2012; 1: 22–31.
23 https://sagdb.uni-goettingen.de/detailedList.php?str_number=40.85 (2020) (accessed 22 April 2020).
24 http://sagdb.uni-goettingen.de/culture_media/05%20Seawater%20Medium.pdf (2020) (accessed 22 April 2020).
25 Fakhri M, Arifin NB, Hariati AM, Yuniarti A. Growth, biomass, and chlorophyll-A and carotenoid content of *Nannochloropsis* sp. strain BJ17 under different light intensities. *Journal Akuakultur Indonesia* 2017; 16: 15–21.
26 Datasheet – Spectroradiometer CS-2000/2000A, www.konicaminolta.com, (2020) (accessed 22 April 2020).
27 https://sphereoptics.de/en/product/zenith-polymer-reflectance-standards/ (2020) (accessed 22 April 2020).
28 CIE Colorimetry. Colorimetry – understanding the CIE system. CIE Colorimetry 1931–2006, 2006.
29 Khanh TQ, Bodrogi P, Vinh QT, Brückner S. *Farbwiedergabe von konventionellen, Halbleiter-Lichtquellen – Theorie | Bewertung | Praxis*. München: Pflaum Verlag, 2013.
30 Khanh TQ, Bodrogi P, Vinh QT, Winkler H. *LED Lighting: Technology and Perception*. New York: Wiley, 2014.
31 Khanh TQ, Bodrogi P, Vinh QT. *Color Quality of Semiconductor and Conventional Light Sources*. New York: Wiley, 2017.
32 https://lumileds.pnwsoft.com/RunPython.aspx?t=3 (2020) (accessed 22 April 2020).

33 DS237-luxeon-sunplus-2835-line-datasheet (2020) (accessed 22 April 2020).
34 Singh SP, Singh P. Effect of temperature and light on the growth of algae species: a review. *Renewable and Sustainable Energy Reviews* 2015; 50: 431–444.
35 https://ams.com/color-sensors (2020) (accessed 22 April 2020).
36 Silicon photodiodes, S1227 series, www.hamamatsu.com (2020) (accessed 22 April 2020).